This article is published as part of a themed issue of ***Photochemical & Photobiological Sciences*** on

Photosynthesis from molecular perspectives – towards future energy production

Guest edited by Suleyman Allakhverdiev, Jorge Casal and Toshi Nagata

Published in issue 2, 2009 of ***Photochemical & Photobiological Sciences***.

Editorial

Perspectives

Papers

Relaxation mechanism of molecular systems containing hydrogen bonds and free energy temperature dependence of reaction of charges recombination within *Rhodobacter sphaeroides* RC

Pavel Mikhailovich Krasilnikov,* Peter Petrovich Knox and Andrew Borisovich Rubin

Received 30th June 2008, Accepted 16th December 2008
First published as an Advance Article on the web 8th January 2009
DOI: 10.1039/b811014j

The mechanism of protonic relaxation is shown to take place in molecular systems containing hydrogen bonds. The mechanism arises from the proton redistribution between two stable states on hydrogen bond lines. This redistribution occurs due to changes of hydrogen bond double well potential, brought about by changes of the electronic state of a molecular system. A characteristic of the relaxation process is that it takes place due to the proton tunneling along hydrogen bonds. The charge shift causes electrostatic potential variation in the electron localization area, which leads to the shift of molecular system energy levels and changes its redox potential. The characteristic time of the protonic relaxation is shown to depend essentially on hydrogen bond bending strain, which increases with the temperature rise and decreases abruptly the efficiency of proton redistribution. Hence, the rate of this process decreases with temperature, in contrast to the activation process. This relaxation process is shown to be responsible for energetic characteristics of recombination reaction $P^+Q_A^- \rightarrow PQ_A$ (free energy difference ΔG and/or reorganization energy λ), temperature dependence in *Rhodobacter sphaeroides* RC.

Introduction

Electron transport in macromolecular biosystems is a fundamental physical process, based on the tunneling effect. Protein-pigment complexes of purple bacteria photosynthetic reaction centers (RCs), the spatial structure of which was obtained using X-ray technology more than 20 years ago,[1,2] are striking examples of systems carrying out such a process. Photoactivation of isolated *R. sphaeroides* RCs causes rapid ($\tau \approx 150$–200 ps) electron transfer within the system of pigment cofactors integrated into apoprotein: bacteriochlorophyll dimer (P) → bacteriopheophytine (I) → primary quinone (Q_A). Then the electron hops to secondary quinone (Q_B) in 150–200 μs[3] In case of the absence of external electron donor and chemically blocked electron transfer to Q_B, or when Q_B is extracted from the RC structure, the process of photooxidised P^+ reduction takes place as a result of the recombination reaction:

$$P^+Q_A^- \rightarrow PQ_A. \quad (1)$$

The reaction (1) is a subject of multiple investigations so far.[4–11] The reaction rate temperature dependence is of particular interest, since it gives one an opportunity to study various relaxation mechanisms that take place within macromolecules as a result of change in electron spatial localization. Within this context the process of electron transfer can be considered as some kind of probe that enables one to get an insight into the mechanisms of molecular machinery functioning.

At room temperature this reaction rate is approximately 10 s^{-1}. During the samples cooling the rate of this reaction is characterized by anomalous temperature dependence—it exhibits a 4–6 fold increase during temperature decrease to cryogenic temperatures. The major change in the rate of the process occurs in the temperature gap 225–175 K.[4–7] It was shown in reference 4 that recombination rate temperature dependence can not be described using conventional theories,[8,9] and additional assumptions should be made to achieve agreement between theory and experimental data. One of the possible assumptions[4,7] that free energy ΔG of the reaction (1) or reorganization energy λ of this process are temperature dependent. Similar assumptions were made in reference 7 to interpret temperature dependence of recombination rate between P and secondary quinone Q_B. In reference 4 a possible temperature dependence of media reorganization energy for reaction (1) was obtained empirically. However, authors in references 4 and 7 pointed out that experimental data do not permit one to distinguish which parameter varies with temperature: ΔG or λ. It can be said confidently only that its sum ($\Delta G + \lambda$) is temperature dependent.

The molecular mechanism which is responsible for the temperature dependence of ΔG or λ is unknown. In this situation the character of this dependence in the temperature gap 175–225 K is of particular interest.[4,5] Obviously experimental behavior of reaction (1) rate temperature dependence is due to some relaxation processes, coupled to electron transfer. In this connection possible conformational changes within protein cofactor environment were discussed in reference 5. In reference 11 an approach taking account of the soft vibration modes in Frank–Condon factor, related to hydrogen bonds dynamics in the primary quinone surrounding, was suggested. We would like to point out that the study of the role of hydrogen bonds in various biological systems is an issue of the day, since these bonds make an essential contribution to structural organization as well as functional operation of molecular systems. The role of hydrogen bonds in photosynthetic RC functioning was fruitfully studied using a site

Lomonosov Moscow State University, Biological Faculty, 119899, Vorobievy Gory, Moscow, Russia. E-mail: krapam@mail.ru

directed mutagenesis approach. An influence of hydrogen bonds formed by dimer P and its environment on P redox characteristics and electron transfer efficiency was studied,[4,7,12,13] as well as electron density distribution between bacteriochlorophylls in the dimer.[14] The influence of hydrogen bonds on redox potential of another system, namely iron–sulfur clusters was studied in reference 15 and 16.

In the present paper we suggest a relaxation process mechanism, which we use for interpretation of temperature dependence of ΔG or λ in reaction (1). This relaxation mechanism is possible only in the case of the molecular system containing hydrogens bonds, and is due to proton redistribution between two stable positions on the double well potential energy surface of a hydrogen bond. This redistribution occurs on changes of hydrogen bond double well potential, stipulated by change of molecular system electronic state, which we regard as appearance or disappearance of an electron in its localization area. A feature of the redistribution process is that it takes place due to tunneling of protons along hydrogen bonds and depends essentially on hydrogen bond bending strain. Temperature rise causes hydrogen bond bending strain to increase due to atoms' thermal motion, and causes abrupt decrease of proton redistribution efficiency. This causes the relaxation process slow down with temperature rise, in contrast to the activation process.

Proton tunneling in the double-welled potential along the hydrogen bond line is equivalent to a charge shift at a distance of 0.6–0.8 Å. Such proton shift influences electrostatic potential, generated by itself in electron localization area. Since a system redox potential is determined by the interactions of valence electron with environmental charges, change of electrostatic potential in electron localization area should cause system redox potential change. Hence the considered mechanism is a process of equilibration in a self consistent system containing an electron and a hydrogen bond proton. Whether this system will reach the true equilibrium or not is determined by the ratio of the system relaxation time, which is referred further as τ, and electron life time at electron binding center τ_e. We will show that the relaxation time τ may vary by many orders of magnitude with temperature variation. Electron life time at primary quinone Q_A is below 0.1 s in case of reaction (1).[4] Hence the true equilibrium within the system will not always be reached during time τ_e. In this connection, the reaction (1) can proceed both as adiabatic and non-adiabatic process at various temperatures. We consider this aspect thoroughly in the appropriate part of our paper.

In the final part of the paper we discuss a possible interpretation of electrostatic interaction energy change in the system electron–hydrogen bond proton during relaxation. On one hand, this energy can be considered as a part of free energy difference ΔG, and on the other hand, as a part of reorganization energy λ for the reaction of recombination $P^+Q_A^- \rightarrow PQ_A$. Finally we compare calculated and empirical[4] reorganization energy temperature dependence. In this part we shall also discuss certain questions important for the correct application of our theory to the concrete reaction (1) that takes place in RC of *Rhodobacter sphaeroides* bacteria. First, it concerns the possibility that hydrogen bonds between Q_A^- and His M219 and also Ala M260 have double well potential. Indeed, recently it has been found that the H-bond between Q_A^- and His M219 is strong,[21] hence it is likely that it is a single well H-bond. This problem is closely related to Q_A^- the head group rotation effect that has been observed[23] recently. We discuss also the possible role of the H-bonds between P^+ and its environment and some other questions. In conclusion, we consider the isotope effect with the H-bond's proton substituted for deuteron.

I. Relaxation mechanism

A. Electrostatic potential variation upon proton transfer along hydrogen bond

Let's consider a molecular system containing hydrogen bonds. The potential energy cross-section profile along a hydrogen bond may contain one or two minima on it.[17,18] In the latter case the profile is called double-welled, and one would say, the hydrogen bond possesses double well potential. A hydrogen bond double well potential is essential for proton transfer along this bond. This process is due to the possibility of tunneling and/or active proton transition between potential wells. In Fig. 1 schematic double well potential energy surface profile along hydrogen bond line is shown. Coordinates of minima are labeled as x_1 and x_2, and correspond to proton stable positions 1 and 2 on the hydrogen bond line.

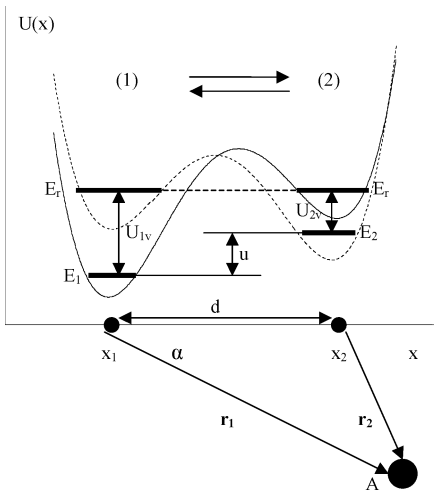

Fig. 1 Schematic depiction of double well profile of potential energy surface crossection along hydrogen bond line x. In case of proton localization at the first minimum (x_1) the ground state energy is E_1, in case of proton localization at the second minimum (x_2) it is E_2. The distance between the potential minima $d = |x_2 - x_1|$. Proton tunneling occurs in the state with energy E_r, which is equienergetic for both proton positions at hydrogen bond line. Difference of the energies of the equilibrium proton positions is denoted as $u = E_2 - E_1$. In order to attain the state with energy E_m the proton should receive the energy U_{1v} from thermostat, when it is localized at the first minimum, or the energy U_{2v} when it is localized within the second potential minimum. The lower part of the figure presents radius vectors $\boldsymbol{r}_1$ and $\boldsymbol{r}_2$, drawn from the centers of proton localization to an observation point A, located within the molecular system. The angle contained by radius vector $\boldsymbol{r}_1$ and hydrogen bond line is denoted as α.

Proton transition from one potential well into another corresponds to charge $+e$ (e, elementary charge) transition at distance $d = |x_2 - x_1|$ along the hydrogen bond line. This charge shift causes change of electrostatic potential magnitude at some point A, which is at distance r_1 from the first minimum and r_2 from the second one (Fig. 1). Further we suppose that electron is localized

about point A. In this figure α denotes an angle contained between the vector $\boldsymbol{r}_1$ and hydrogen bond line. Due to partial screening by electron density of a covalent bond, to the external observer proton charge appears to be equal to some quantity e_p, the so called effective partial charge. In most cases partial charge e_p belongs to an interval $0.3e \leq e_p \leq 0.5e$. When the proton is localized in j-th ($j = 1, 2$) minimum, it produces electrostatic potential

$$\varphi_j = \frac{e_p}{\varepsilon r_j}, \tag{2}$$

where ε denotes media permittivity.

Let's denote populations of the first and the second potential wells as $n_1(t)$ and $n_2(t)$. These quantities depend on time t and describe the probability of proton localization in the corresponding minimum. Electrostatic potential generated by the proton charge at point A can be expressed as

$$\varphi(A,t) = n_1(t)\varphi_1 + n_2(t)\varphi_2. \tag{3}$$

To get an explicit form of function (3) one should find an explicit form of n_1(t) and n_2(t) time dependencies. In Fig. 1 bold horizontal lines denote energy ground levels of the system in case of proton localization in the first (E_1) and second (E_2) potential wells. Energy difference of these states is denoted as $u = E_2 - E_1$. The proton can transit between the wells only when the energy difference u is compensated as a result of interaction between proton and environment. For example, the compensation may be due to interaction between the proton and vibrations of the molecular system. Proton tunneling between wells can be qualitatively described as follows (see Fig. 1). At the starting moment the proton localized in the first well gains additional energy U_{1v} due to interaction with vibrational modes of the molecule and reaches some intermediate state with energy $E_r = E_1 + U_{1v}$, which is equi-energetic to state with energy $E_r = E_2 + U_{2v}$ in case of proton localization in the second well. This intermediate state satisfies the resonance condition for energy levels, *i.e.* is degenerate. Under this condition the proton tunneling from the first well to the second one is possible. The probability of proton tunneling per time unit is denoted as k_0. The quantity $\tau_0 = (k_0)^{-1}$ denotes an average life time of the proton within a well. If a transitional state lives long enough compared to τ_0, the quantum oscillations will arise and proton will hop between the wells back and forth. These oscillations correspond to proton delocalization between these two positions. If proton life time within the second well is enough for dissipation of excessive energy U_{2v}, for example due to interaction with vibrational modes of the system, the proton will be localized in the second well with energy E_2.

Let us point out, that vibrational energy U_{1v} absorbed by the proton can not be less than the energy u, *i.e.* $U_{1v} \geq u$. Since we do not make any assumptions concerning the magnitude of U_{jv} ($j = 1, 2$), the processes of vibrational energy absorption and emission by the proton due to interaction with environment should be considered as a multi-phonon process.[19] It permits one to use the Boltzmann distribution to calculate the population of the corresponding states, at a good level of approximation.

As a result, kinetic of proton tunneling between potential wells can be described using a conventional approach, describing this process as a forward and backward reaction with rate constants k_1 and k_2, respectively. In case of potential presented at Fig. 1, forward reaction (1) $\rightarrow$ (2) rate constant k_1 and backward reaction (1) $\leftarrow$ (2) rate constant can expressed as follows:

$$k_1 = k_0\exp(-U_{1v}/k_bT),\ k_2 = k_0\exp(-U_{2v}/k_bT), \tag{4}$$

where k_0 is the above mentioned factor, accounting for the rate of proton tunneling, or in other words, a probability of proton transition per time unit in case of energy balance (*i.e.* when the system is in a state with energy E_r), k_b Boltzmann factor, T absolute temperature.

Populations n_1(t) and n_2(t) are related due to normality condition:

$$n_1(t) + n_2(t) = 1 \tag{5}$$

Expressions for populations $n_1(t)$ and $n_2(t)$ can be found by solving the following system of equations:

$$\begin{cases} \dot{n}_1 = -k_1 n_1 + k_2 n_2 \\ \dot{n}_2 = -k_2 n_2 + k_1 n_1 \end{cases}, \tag{6}$$

where the point denotes time differentiation. Using eqn (6) and entry conditions $n_1(0) = n_{01}$, $n_2(0) = n_{02}$, one can find:

$$n_1(t) = n_{01}\exp\{-t/\tau\} + (1 + K)^{-1}(1 - \exp\{-t/\tau\}), \tag{7}$$

where $K = k_1/k_2 = \exp(-u/k_bT)$ is an equilibrium constant, $\tau = (k_1 + k_2)^{-1}$ is relaxation time. The expression for n_2(t) can be easily obtained using (5) and (7). Relaxation time τ, which plays an essential role in further discussion can expressed as:

$$\tau = k_0^{-1}(1 + \exp\{-|u|/k_bT\})^{-1}\exp(\mu_{ph}/k_bT). \tag{8}$$

Here $\mu_{ph} = U_{2v}$ denotes an energy of absorbed phonons (vibrational quantum), which is required by the proton to reach the state with energy E_r, when it is located within the well with higher energy level. Let us point out that contrary to the expression for equilibrium constant, expression (8) contains modulus $|u|$. This is dictated by the ease of use of the equation (8) for different potential energy profiles, since the state with energy E_r, which is essential for tunneling, is always an activation process no matter which of the potential wells is the deepest one. Finally one has to calculate the constant k_0, to determine relaxation time, and we address this problem in the next section.

Now let us pay attention the fact that the potential energy profile of a hydrogen bond can vary.[11] This can happen, for example, upon change of the electronic state of the molecular system, which we regard as appearance or disappearance of an electron in its localization area at Q_A molecule. These changes may influence energetic parameters of the potential as well as its shape. Hydrogen bonds between primary quinone Q_A and histidine (His(M219)), and Q_A and dipeptide (Asn(259)–Ala(M260)) were shown[11] to change the shape of their potential energy profiles from single-welled to double-welled upon primary quinone reduction. Difference u of the equilibrium energies of the system during proton localization within different wells, is an energy parameter that characterizes possible changes of hydrogen bond potential. Further we use this difference to characterize possible change of the hydrogen bond potential and denote it as u_1 in the initial state of the system, and u_2—in the final state, that is—after change of an electronic state of the system. There are two possible relations between these parameters, which determine qualitative as well as

quantitative differences of protonic kinetics: (1) $u_1 > 0$, $u_2 > 0$; (2) $u_1 > 0$, $u_2 < 0$. In the first case, the first potential well is deeper than the second one at the initial state as well as after the change of the system electronic state, however energy levels E_1 and E_2 probably shift relative each other, since generally $u_1 \neq u_2$ (see Fig. 4a,b). In the second case, the second well becomes deeper than the first one upon change of the system electronic state, while the first well is deeper at the initial state (Fig. 4d,c). Cases (3) $u_1 < 0$, $u_2 < 0$ and (4) $u_1 < 0$, $u_2 > 0$ differ from the cases discussed above only in placement of the observation point A relative the hydrogen bond, which is determined by the value of angle α (Fig. 1). In cases when $\alpha < \pi/2$, the first variant takes place, in cases when $\alpha > \pi/2$ it is the third one. The same rule applies to variants 2 and 4 respectively.

Using eqn (7), one can write an expression for $n_1(t)$ time evolution upon change of the system electronic state. Let us denote the difference of the proton energy levels within different wells as u_1 at the initial state, and u_2 after change of the system electronic state, then:

$$n_1(t) = (1 + K_1)^{-1}\exp(-t/\tau') + (1 + K_2)^{-1}(1 - \exp\{-t/\tau'\}), \quad (9)$$

where $n_1(0) = (1 + K_1)^{-1}$, $K_1 = \exp[-u_1/k_bT]$ is an equilibrium constant at the initial state, and $K_2 = \exp[-u_2/k_bT]$ is an equilibrium constant at the final state. The expression (9) is obtained under condition of the instantaneous change of the electronic state. Therefore, $t \leq 0$ corresponds to the equilibrium populations of n_{10} and n_{20} in the initial electronic state, *i.e.* according to eqn (7), $n_{10} = n_1(\infty) = (1 + K_1)^{-1}$. After the change of the electronic state, *i.e.* $t > 0$, the evolution of the populations in this final electronic state proceeds. In general in the final electronic state the values of parameters u and u_{ph} also changes. Hence, in this cause the magnitude of τ' can differ from the τ value in (8), as well. In view of this remark we subsequently shall keep symbol τ for the relaxation time.

Taking into account eqn (7), we can now express the electrostatic potential (3), generated by the proton charge at the observation point:

$$\varphi(A,t) = n_1(t)(\varphi_1 - \varphi_2) + \varphi_2. \quad (10)$$

It should be noted that potentials φ_1 and φ_2 are independent of the electronic state according to its definition in eqn (2).

Let's suppose that the electron localizes within some area centered at point A, for example it localizes at primary quinone Q_A. The redox potential, which characterizes system electronic structure, includes the energy due to interaction between the electron and the proton:

$$E_m = -e\varphi(A,t) \quad (11)$$

An electron traveling the electron transfer pathway lives at this center for the finite time τ_e. So, redox potential $E_m(\tau_e)$, which relaxes during time τ_e due to environment relaxation, may be different from its equilibrium value $E_m(t \to \infty) = E_{m0}$, *i.e.* in general case $E_m(\tau_e) \neq E_{m0}$. The relation between these values is determined by the relation between the environment relaxation time and electron life time at this accepting center. If it takes place the inequality $\tau_e << \tau$ is valid and then the electron transfer is an non-adiabatic process; in the opposite case, $\tau_e >> \tau$, this process is adiabatic. As is well known this classification is connected with the nuclear tunneling. We address this problem below.

According to eqn (10), we express the value of electrostatic potential at observation point at time t relative its value at this point at the starting moment:

$$\Delta\varphi(A,t) = \Delta\varphi(A,t) - \varphi(A,0) = (\varphi_2 - \varphi_1)\lfloor(1 + K_1)^{-1} - (1 + K_2)^{-1}\rfloor[1 - \exp\{-t/\tau\}]. \quad (12)$$

The quantity ΔE_m, which equals

$$\Delta E_m = -e\Delta\varphi(A,t) \quad (13)$$

determines shift of the electron accepting center energy levels, due to interaction between this electron and hydrogen bond proton. This is an essential parameter which can play a key role in the process of the system fine tuning for establishing an electron tunneling between accepting centers (from donor at acceptor). Below we address this aspect thoroughly, as well.

B. Proton tunneling within two well potential (calculation of k_0)

In order to complete the description of electrostatic potential evolution during protonic relaxation, one should find an explicit expression for the parameter k_0, which determines the probability of proton tunneling between the wells within hydrogen bond double well potential. In order to calculate the value of k_0 in case of symmetric model potential, which corresponds approximately to the state of a hydrogen bond with the energy E_r, we consider model double well potential $U(x)$, which is defined as follows:

$$U(x) = \begin{cases} U_1(x) = \frac{1}{2}m\omega^2(x + \frac{d}{2})^2, & x \leq 0, \\ U_2(x) = \frac{1}{2}m\omega^2(x - \frac{d}{2})^2, & x \geq 0, \end{cases} \quad (14)$$

where m denotes a proton mass, ω frequency of a proton vibrations within potential well, $\pm\frac{d}{2}$ the locations of the potential minima on a hydrogen bond line (the starting-point of coordinate system is the middle of segment x_1x_2 (Fig. 1)). According to (14) the model potential $U(x)$ is a superposition of two hemiparabolas. We suppose that the proton energy within either well satisfies the condition $E_r << U(0) = 1/2m\omega^2(d/2)^2$, *i.e.* is much less than the height of the potential barrier separating the wells. Under this assumption we can describe proton localization within a separate well as if it were localized within a pure parabolic well. Furthermore, for the sake of simplicity we suppose the energy of the proton to be equal $E_r = 1/2\hbar\omega$, *i.e.* energy of the harmonic oscillator ground level. Since the solution of the Schroedinger equation describing the harmonic quantum oscillator is a well known result, we can write out this solution for the wells 1 and 2 in case of isolated harmonic potential wells:

$$\hat{H}_j\Psi_j = \varepsilon_0\psi_j, j = 1, 2, \quad (15)$$

where Hamiltonian $\hat{H}_j = \hat{T} + U_j$, $\hat{T}$ denotes an operator of kinetic energy, $\varepsilon_0 = E_r = 1/2\hbar\omega$ is a quantum oscillator ground state energy. At ground state, eigenfunctions of operators $\hat{H}_j$ are as follows:

$$\psi_1(\xi) = \pi^{-1/4}\exp\left(-\tfrac{1}{2}(\xi + \delta)^2\right),\ \psi_2(\xi) = \pi^{-1/4}\exp\left(-\tfrac{1}{2}(\xi - \delta)^2\right), \quad (16)$$

where $\xi = \frac{x}{x_0}$ is a dimensionless coordinate, $\delta = \frac{d/2}{x_0}$ is a dimensionless position of the potential minimum on ξ axis, $x_0 = \sqrt{\frac{\hbar}{m\omega}}$ is the magnitude of the proton zero-point oscillations.

For the complete system of joined potential wells the following expression for the Hamiltonian holds

$$\hat{H} = \hat{T} + U_1 + U_2 = \hat{H}_1 + U_2 = \hat{H}_1 + U_2 = \hat{H}_2 + U_1. \quad (17)$$

Since wave functions (16) are not eigenfunctions of Hamiltonian (17), the states described by them are stationary, *i.e.* they change with time. In order to find time dependence of these states, we consider non-stationary Schroedinger equation with Hamiltonian (17)

$$i\hbar\frac{\partial\psi}{\partial t} = \hat{H}\psi. \quad (18)$$

We express wave function ψ as a linear combination

$$\psi(t) = a_1(t)\psi_1 + a_2(t)\psi_2. \quad (19)$$

Coefficients $a_j(t)$ in states superposition (19) are the weight factors, that determine the probability $p_j(t)$ of state ψ_j realization: $p_j(t) = |a_j(t)|^2$. Using the standard method of variations we obtain the following expressions for $p_j(t)$ (see Appendix A):

$$\begin{cases} p_1(t) = |a_1|^2 = \frac{1}{2}\left(1 + \cos(\pi k_0 t\right), \\ p_2(t) = |a_2|^2 = \frac{1}{2}\left(1 - \cos(\pi k_0 t\right), \end{cases} \quad (20)$$

where

$$k_0 \approx \frac{2\nu}{\sqrt{\pi}}\delta \times \exp(-\delta^2). \quad (21)$$

Here $\nu \equiv \nu_H = \omega/2\pi$ denotes frequency of proton linear oscillations within a well, and $\delta = \frac{d/2}{x_0}$ ($d/2$ is equal to the half distance between two minimums of the double well potential). If a hydrogen bond is formed by deuterium D then other parameters provided being the same the frequency is $\nu_D = \frac{1}{\sqrt{2}}\nu_H$.

Formula (21) is an approximate expression for proton tunneling probability, since, first, we did not take into account excited states of the oscillator, and, second, the real potential can be approximated by a harmonic one only in the vicinity of the potential minimum. Hence, the values of k_0, calculated using formula (21) should be regarded as order of magnitude estimations. The expressions (21) and (8) fully determine relaxation time τ within hydrogen bond double well potential.

C. Hydrogen bond strain

We have considered the process of proton tunneling along a hydrogen bond within double well potential. We also have made a default assumption, that the proton locates on the line connecting two electronegative atoms, which form the hydrogen bond. This is the case of the so-called strainless hydrogen bond. In this case it is the most strong hydrogen bond.[17] However, in real environments thermal motion of atoms or conformational changes may cause reorientation of molecules or their fragments. This may cause a relative shift of molecule fragments, forming a hydrogen bond. As a result, the hydrogen bond is strained or even torn. We are interested in hydrogen bond bending strain, which corresponds to the shift of a proton from the line connecting two electronegative atoms which form the bond (Fig. 2). This strain causes changes in hydrogen bond parameters, hence altering the probability of proton tunneling and relaxation time.

One of the most evident consequences of hydrogen bond bending strain is an increase of distance between double well potential minima. In other words, hydrogen bond strain increases the width of energy barrier separating potential wells. Fig. 2

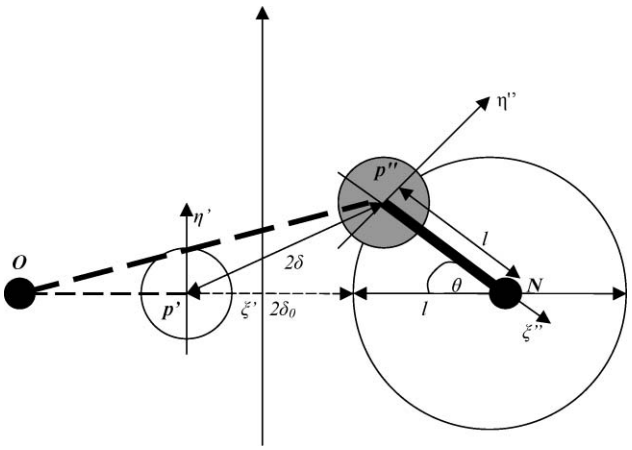

Fig. 2 Schematic depiction of a strained hydrogen bond $O\cdots H$–N, formed by the electronegative oxygen O and nitrogen N atoms. Notation: l, covalent bond length H—N; $2\delta_0$, the distance between the potential minima of strainless hydrogen bond; θ, angle of hydrogen bond strain. Circles labeled with p, two proton localization areas. Dark circle, current proton localization. Dashed line Op denotes hydrogen bond. Coordinate planes (ξ', η') and (ξ'', η'') describe the space of two-dimensional harmonic oscillations of a proton within localization area (see in text).

presents the scheme of strain of a hydrogen bond formed by molecular fragments R_1–O–H–N–R_2 (R_1 and R_2 are not shown, O, H, N denote oxygen, hydrogen and nitrogen atoms respectively). The following notation is used in the figure: circles p', p'' denotes proton localization area within double well potential of strained hydrogen bond; gray circle p'' denotes an area where the proton is being localized now; l is the length of H–N covalent bond; $2\delta_0$ is the distance between potential minima in case of strainless hydrogen bond; 2δ is the same distance in case of strained hydrogen bond; θ is strain angle, *i.e.* angle contained by covalent bond H–N and line connecting proton and nitrogen atom ON. Using triangle $Op''N$ (Fig. 2) one can obtain an expression for the distance 2δ between potential minima as a function of angle θ:

$$\delta(\theta) = \left[\delta_0^2 + (2\delta_0 + l) \times l\sin^2(\theta/2)\right]^{\frac{1}{2}}. \quad (22)$$

Since expression (22) is an exponential factor of expression (21), even slight variations of angle θ may cause considerable increase of characteristic tunneling time of a proton, and hence increase of relaxation time (8).

Note that expression (21) was obtained for the case of one-dimensional potential (coordinate is x or ξ) along hydrogen bond line. This potential is a potential energy surface profile cross-section which can be obtained as a result of potential energy surface dissection along hydrogen bond line (reaction coordinate). In general, we should consider the tunneling process in three-dimensional space in case of a strained bond. Suppose that proton is located within three-dimensional harmonic potential well (ξ, η, ζ are spatial coordinates), and proton vibrations along each coordinate are of the *same* frequency. In this case the problem of proton tunneling in three-dimensional space is analogous to the problem considered above. Though in this case potential energy dissection is made along the line, connecting centers of proton localization, *i.e.* along the line $p'p''$ (Fig. 2).

Now we discuss the problem of possible hydrogen bond deformation mechanisms. The evident factor is a thermal motion of atoms and molecules. Temperature is a measure of the intensity of atoms motion. The increase in temperature always causes thermal expansion of bodies (except some rare cases, for example water in temperature gap 0–4 °C). It is a consequence of atom motion intensification, which may be characterized as an increase of average interatomic and intermolecular distances. The less strong a bond the more elongation it undergoes. For example in case of hydrogen the following equation holds:

$$\delta_0(T) = \delta_0(0)(1 + \alpha_t \mathrm{T}), \tag{23}$$

where α_t is a factor of thermal expansion, T the absolute temperature.

Within a condensed medium, the types of molecular motions that cause periodic changes of molecular groups relative orientation are torsional and librational vibrations. These degrees of freedom correspond to free molecules rotational degrees of freedom. Average energy that falls at single degree of freedom equals $1/2\ k_b T$. Denoting hydrogen bond bending strain rigidity as g ($[g] = \mathrm{J\ rad^{-2}}$), one can obtain an expression for average angle of deviations of librational oscillator during its period

$$\langle\theta\rangle \approx \sqrt{\frac{k_b T}{2g}}. \tag{24}$$

It follows from (23) and (24), that effective distance between potential minima of a hydrogen bond under stress (effective width of the barrier) changes with temperature of the medium. Hence factor k_0 (21) and protonic relaxation time τ (8) are temperature dependent.

As we have noted above, hydrogen bond deformation can be caused not only by molecular thermal motion, but also by conformational changes of molecular structure. Let us suppose that in first conformation a hydrogen bond is strainless, and in the second one it is distorted by angle θ_C. In this case, the state of the bond is determined by the activative process of transitions between the conformations. These transitions can be described using a theory of transition complex. The kinetic scheme that describes changes of conformational states populations N_1 and N_2 is analogous to the scheme (6). Based on this, one can derive an expression for parameter $\langle\delta(\theta_C)\rangle$:

$$\langle\delta(\theta_C,t)\rangle = N_1\delta_0 + N_2\delta(\theta_C) = \delta(\theta_C) - N_1(\delta(\theta_C) - \delta_0), \tag{25}$$

where time evolution τ_r of population of conformational state 1 (*i.e.* conformation that corresponds strainless hydrogen bond) is analogous to expression (7):

$$N_1(t) = N_{10}\exp(-t/\tau_r) + (1 + K_C)^{-1}(1 - \exp(-t/\tau_r)). \tag{26}$$

Here K_C denotes equilibrium constant of conformational transition, which is determined by free energy difference ΔG_C of corresponding states

$$K_C = \exp(-\Delta G_C/k_b \mathrm{T}). \tag{27}$$

If a change of electronic state of a molecular system causes change of a potential energy surface profile along conformational coordinate, the expression (33) transforms to an expression analogous to (9):

$$N_1(t) = (1 + K_{C1})^{-1}\exp(-t/\tau_r) + (1 + K_{C2})^{-1}(1 - \exp(-t/\tau_r)), \tag{28}$$

where K_{C1} and K_{C2} are constants of equilibrium (27) determined by corresponding free energy differences ΔG_{C1} and ΔG_{C2}.

The mechanisms of hydrogen bond deformation due to libration of molecules and due to conformational changes are essentially different from each other. The first one is universal by nature; it takes place in any system and causes a wide range of hydrogen bonds deformations. On the contrary, the second one occurs only upon conformational change and causes deformation of a distinct magnitude—the angle θ_C. We do not discuss thoroughly the conformational mechanism of hydrogen bond strain here, since we suppose to discuss it in separate paper. In the current paper we confine the discussion to mechanism of librational distortions only (24) taking into account media thermal expansion (23).

II. Parameters general analysis

The values of relaxation time τ, electrostatic potential at a fixed point of a system φ and change of this potential during relaxation $\Delta\varphi$ depend on many parameters. We are going to discuss them and find the most critical.

A. Relaxation time τ

According (8), (21)–(24) the value of protonic relaxation time τ depends on ν, l, δ_0, α_t, g, u, u_{ph}, T. Now we discuss them sequentially.

Frequency ν of proton vibrations within the well corresponds to the frequency of its valence vibrations. According experimental measures its values belong the range $1.05–0.75 \times 10^{14}\ \mathrm{s^{-1}}$. Hence, the magnitude of proton zero-point vibrations belong the range $0.098 \le x_0 \le 0.116$ Å, so we take it to be equal $x_0 \approx 0.107$ Å.

The length of covalent bonds between hydrogen atom and oxygen or nitrogen atoms (H–O, H–N) can be supposed to be constant and equals $l = 1$ Å. Distance d between double well potential minima can be assessed based on the data for distances R between electronegative atoms forming the hydrogen bond. Typical values are from 2.7 up to 3.1 Å. Hence distance d lies within an interval $0.7 < d < 1.1$ Å and parameter $\delta_0 = 0.5d/x_0$ belongs in the interval $3.3 < \delta_0 < 5.1$. For our estimations we take $\delta_0 = 4$.

According to data[20] obtained using high resolution NMR techniques, the linear thermal expansion factor of a hydrogen bond equals $\alpha_t = 1.7 \times 10^{-4}\ \mathrm{K^{-1}}$. During a temperature increase from 0 to 300 K, hydrogen bond length increases only by 5%. Although the effect is small it is worth accounting for, since parameter δ is contained in exponential factor of expression (21).

Hydrogen bond bending strain rigidity g is the most poorly defined parameter. Estimation of its order of magnitude is based on the data for frequencies of rotational and deformational vibrations of molecules forming hydrogen bonds: $g = I\omega^2$, where I denotes moment of inertia of a molecule and frequency ω equals either the frequency of rotational vibrations ω_t or the frequency of deformational vibrations ω_β. Frequencies of rotational vibrations belong an interval $27–9 \times 10^{12}\ \mathrm{s^{-1}}$, and frequencies of deformational vibrations are less than $\omega_\beta < 1.5 \times 10^{12}\ \mathrm{s^{-1}}$. Broad absorption bands corresponding to these vibrations are registered within various media, for example in water. Using the value of the water molecule moment of inertia we estimated the value of parameter g to be in the range $10^{-21} \le \mathrm{g} \le 10^{-19}\ \mathrm{J\ rad^{-2}}$ (or $0.6 \times 10^{-2} \le \mathrm{g} \le 0.6\ \mathrm{eV\ rad^{-2}}$).

The value of the energy gap u as well as the energy of absorbed phonons u_{ph} are also undefined variables. However parameter u causes minor changes of relaxation time. Actually, according (8), change of u from 0 to ∞ causes only a twofold change of time τ. Hence we postpone the discussion of this parameter until discussion of electrostatic potential, where it plays an essential role. It is quite hard to tell something about u_{ph} value confidently. If the condition $u_{ph} >> k_bT$ holds true, the value of u_{ph} may become critical. Although, taking into account high spectral density of vibrational modes of polyatomic systems we suppose it to be comparable with k_bT: $u_{ph} \sim k_bT$. Since we estimate just the order of magnitude of the relaxation time, this assumption is quite reasonable. It is possible to give some arguments in favor of this assumption. According to (8), (21), (22) and (24), the following approximation at the condition $\theta << 1$ is true:

$$\tau \propto \exp\left((2\delta_0 + l)l\frac{k_bT}{8g} + \frac{u_{ph}}{k_bT}\right)$$

The value of τ is minimal at $u_{ph} = \frac{(2\delta_0 + l)l}{8}\frac{k_bT}{g}k_bT$. Hence, for the process of protonic relaxation to be effective, it is necessary to fulfil the condition $u_{ph} < nk_bT$, where n is equal to several units. If we accept that u_{ph} is constant we obtain non-monotonic temperature dependence of the relaxation time. We have discussed an analogous problem early.[11]

The last parameter, announced above, is a medium temperature. In general, temperature is an important factor, which enables one to make a qualitative comparison of calculated parameters with experimentally measured ones and make some conclusions about validity of used assumptions.

Fig. 3 presents the dependence of $\log_{10}(\tau/[s])$ on the value of hydrogen bond bending strain rigidity g (a) as well as on temperature (b). Fig. 3(a) presents curves for four temperature values: 1–30, 2–100, 3–200, 4–300 K. As one can see, relaxation time τ depends on hydrogen bond bending strain rigidity in a crucial fashion. For example, at temperature 300 K (curve 4) change of g by 1 order of magnitude causes a change of τ by 30 orders of magnitude. Even at $T = 30$ K (curve 1), protonic relaxation time changes by several orders of magnitude. Thus the process of protonic relaxation is very sensitive to this characteristic of hydrogen bond.

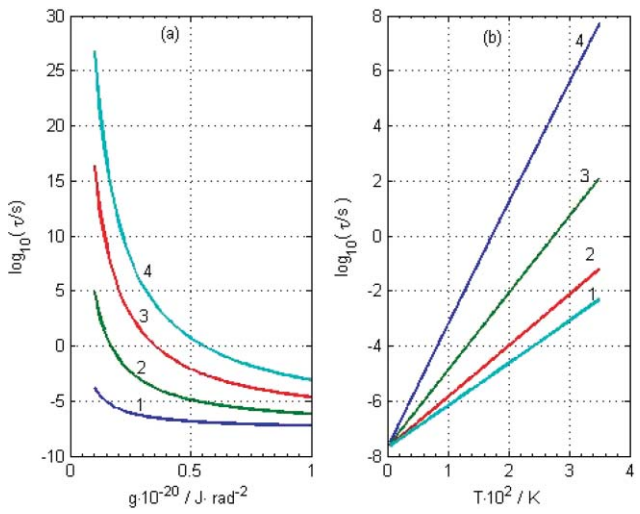

Fig. 3 The dependence of $\log_{10}(\tau/s)$ (see in text) on the value of hydrogen bond bending strain rigidity g (a) and on temperature (b). The curves in subplot (a) are presented for four different temperature values: 1–30, 2–100, 3–200, 4–300 K. The curves in subplot (b) are presented for four different values of parameter g: 1–1 × 10^{-20}, 2–0.8 × 10^{-20}, 3–0.5 × 10^{-20}, 4–0.3 × 10^{-20} J rad^{-2}.

Fig. 3(b) presents curves for three values of parameter g: 1–1 × 10^{-20}; 2–0.8 × 10^{-20}; 3–0.5 × 10^{-20}; 4–0.3 × 10^{-20} J rad^{-2}. According to the presented curves, temperature change from 5 to 350 K causes a change of protonic relaxation time by several orders of magnitude. For example, when g = 0.3 × 10^{-20} J rad^{-2} relaxation time changes almost by 15 orders of magnitude (curve 4). The more rigid the hydrogen bond the less are the changes in protonic relaxation time (see curve 1). When the rigidity is about 5 × 10^{-20} J rad^{-2}, relaxation process due to hydrogen bond bending strain is virtually stopped.

Using these estimations, one can say that the most crucial parameter is hydrogen bond bending strain rigidity g. Another crucial parameter is a medium temperature T. The parameter u_{ph} is not crucial, unless its value is larger than several k_bT.

B. The electrostatic potential φ

Now we discuss electrostatic potential (10) and (12). The value of electrostatic potential at the observation point depends mainly on the value of partial charge of the proton e_p. We have already noted above that the value of a proton partial charge is determined by spatial electron density distribution of a molecule upon formation of a covalent bond between electronegative atom and the proton. According to quantum chemical calculations e_p values varies from 0.3 e up to 0.5 e (e, elementary charge). For our estimations we use the value $e_p = 0.4\ e$.

We suppose geometrical parameters r_1, r_2 and angle α, contained by the vector $\boldsymbol{r}_1$ and the line of a strainless hydrogen bond, to be temperature independent, since we suppose that the condition $|\boldsymbol{r}_{1,2}| >> d$ holds, where d denotes distance between hydrogen bond potential minima (Fig. 1). These parameters are determined by molecular structure and we suppose them to be constant. In this connection it is worth noting that the most probable participants of the relaxation process are hydrogen bonds within the closest environment of an electron accepting center as well as hydrogen bonds within water clusters in the neighbourhood of an electron accepting center. Further we suppose that the closest environment implies the structure contained by the spherical region with radius 15–20 Å and centered at the center of an electron localization area. We also suppose that distances from electron localization area center and protons of hydrogen bonds belong to the interval $3 \le |\boldsymbol{r}| \le 15$ Å. The angle α (Fig. 1) has any value. Hence we use for numerical estimations the value $\langle \cos^2\alpha \rangle = \frac{1}{2}$.

Media dielectric permeability ε is also an important parameter. In the case of biological molecular systems, dielectric permeability implies static dielectric permeability. Its value is supposed to be equal to some average macroscopic value, which characterizes certain media. For example, in the case of water solutions it is supposed to be equal to 80, and in the case of proteins or membranes it is 2–5. However one should note that biological media are highly heterogeneous. Hence local values of ε may vary considerably across the system. Furthermore, one should note, that dielectric permeability of a biological medium due to dipole orientational mechanism of polarization possess a dispersion in

frequency interval from 10^7 to 10^{12} Hz. Hence in the case of processes with characteristic times in pico- or nanosecond range one should take into account medium inertia. Since a medium inertia property depends on temperature, the value of ε depends on temperature as well. Hence $\varepsilon = \varepsilon(\boldsymbol{r}, \omega, T)$. In reference 10 it was shown that the part of the medium reorganization energy λ_o is compensated due to relaxation process of medium dielectric permeability upon electron transfer reaction

$$\lambda_o = e^2\left(\frac{1}{\varepsilon_\infty} - \frac{1}{\varepsilon_s}\right)\left(\frac{1}{2r_1} + \frac{1}{2r_2} - \frac{1}{2r_{12}}\right)$$

where ε_∞ denotes dielectric permeability at high frequencies; it is often supposed to be equal $\varepsilon_\infty = n^2$, where n denotes medium optical refraction factor, which is due to electronic polarization of molecules; ε_s denotes static dielectric permeability; r_1 and r_2 are the radii of the reactants; r_{12} is the distance between the centers of the reactants. Thorough consideration of biological medium polarization mechanisms goes beyond the limits of this paper, since it demands a special discussion. Further we suppose dielectric permeability to be constant and equal $\varepsilon = 4$.

As we have noted above, the less defined parameter is the parameter u, which characterizes energy difference between the states when the proton is localized within different wells of a hydrogen bond double well potential (Fig. 1). Fig. 4 presents possible changes of a molecular system potential surface profile along the hydrogen bond line upon change of the system electronic state. The first case corresponds to a profile transition from shape (a) to shape (b) (see Fig. 4). During this transition energy levels shift, however the energy level of the first well remains the lower one, *i.e.* the following condition for energy levels difference holds: $u_1 > 0$ and $u_2 > 0$. The second case corresponds to profile transition from shape (c) to shape (d) (see Fig. 4). In this case the energy level of the first well shifts upward relative to the energy level of the second well in reply to a change of system electronic state, *i.e.*

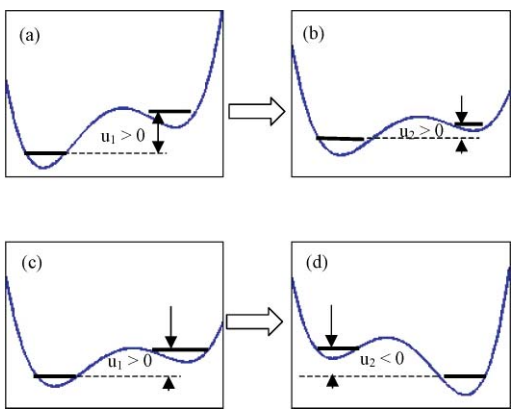

Fig. 4 The scheme illustrating possible changes of system potential energy surface profile along the hydrogen bond, due to a change of system electronic state. The first case corresponds to a profile transition from shape (a) to shape (b). During this transition energy levels shift, however energy level of the first well remains the lower one, *i.e.* the following condition for energy levels difference holds: $u_1 > 0$ and $u_2 > 0$. The second case corresponds to profile transition from shape (c) to shape (d). In this case the energy level of the first well shifts upward relative to the energy level of the second well upon change of system electronic state, *i.e.* $u_1 > 0$ and $u_2 < 0$.

$u_1 > 0$ and $u_2 < 0$. These changes of a hydrogen bond potential cause changes in a potential well's populations relative to its initial values, which is described by the formula (9). Numerical values of parameters u_1 and u_2 are not limited by any condition. If $|u_{1,2}| >> k_bT$, single well hydrogen bond potential exists. Observable variations of electrostatic potential (10) may take place only under the condition $|u_2| < 0.5$ eV, while starting conditions, *i.e.* the value of $|u_1|$, do not play any role.

Let us illustrate the character of temperature dependence of electrostatic potential variations at an observation point using several examples. Fig. 5 presents an illustration of electrostatic potential $\varphi(A)$ temperature dependence at observation point A, which is 5 Å aside from the hydrogen bond proton (the angle $\alpha = 30°$). The curves correspond to the first case of hydrogen bond potential profile change, which corresponds to (a) → (b) transition (Fig. 4): $u_1 = 0.1$ eV → $u_2 = 0.05$ eV. An electron lifetime at electron accepting center, which limits the time of protonic relaxation, equals $\tau_e = 0.1$ s. Different curves correspond to different hydrogen bond bending strain rigidity: 1, $g = 0.1 \times 10^{-20}$; 2, $g = 0.3 \times 10^{-20}$; 3, $g = 0.5 \times 10^{-20}$; 4, $g = 0.7 \times 10^{-20}$ J rad^{-2}. Non-monotonic character of $\varphi(T)$ dependence is due to a decrease of the second well population upon intensification of backward proton transitions with temperature rise. At the same time, due to hydrogen bond strain increase at high temperatures, this curve gradually passes into the curve for small rigidity. At high

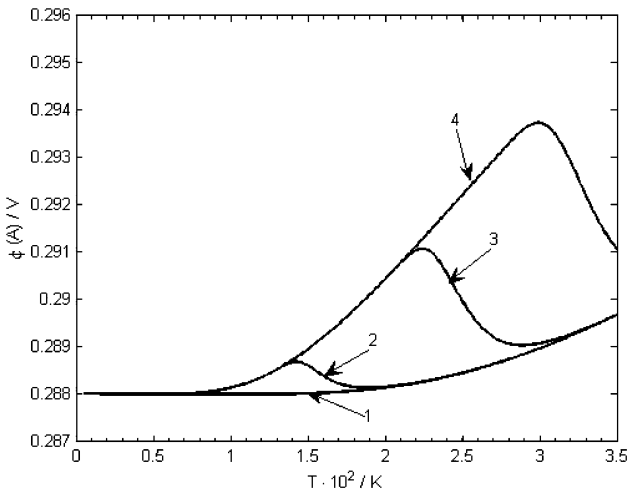

Fig. 5 The figure illustrates electrostatic potential $\varphi(A)$ temperature dependence at observation point A, which is 5 Å aside from the hydrogen bond proton (angle $\alpha = 30°$). The curves correspond to the first case of hydrogen bond potential profile change, which corresponds to (a) → (b) transition (Fig. 4): $u_1 = 0.1$ eV → $u_2 = 0.05$ eV. An electron lifetime at electron accepting center, which limits the time of protonic relaxation equals $\tau_e = 0.1$ s. Different curves correspond to different hydrogen bond bending strain rigidity: 1, $g = 0.1 \times 10^{-20}$; 2, $g = 0.3 \times 10^{-20}$; 3, $g = 0.5 \times 10^{-20}$; 4, $g = 0.7 \times 10^{-20}$ J rad^{-2}. Non-monotonic character of $\varphi(T)$ dependence is due to decrease of the second well population upon intensification of backward proton transitions with temperature rise. At the same time, due to hydrogen bond strain increase at high temperatures, this curve gradually passes into the curve, that corresponds the case of small rigidity. Hence, at high temperatures electrostatic potential varies mainly due to relaxation under condition of strained hydrogen bond. This, in turn, is due to considerable dependence of protonic relaxation time on hydrogen bond bending strain and temperature (Fig. 3(a,b)).

temperatures electrostatic potential varies mainly due to relaxation under condition of strained hydrogen bond. This, in turn, is due to considerable dependence of protonic relaxation time on hydrogen bond bending strain and temperature (Fig. 3(a,b)). With the rise of parameter g value, the magnitude of potential change increases, and curve maximum shifts toward high temperatures region. For example, the maximum of curve 3 is located at 220 K, and the value potential changes magnitude equals 3 mV.

Fig. 6 presents an illustration of electrostatic potential $\varphi(A)$ temperature dependence at observation point A in the case of hydrogen bond potential profile transition (c) → (d) (Fig. 4): $u_1 = 0.1$ eV → $u_2 = -0.05$ eV. An electron lifetime at the electron accepting center, which limits the time of protonic relaxation, equals $\tau_e = 0.1$ s. Different curves correspond to different hydrogen bond bending strain rigidity, just like in the case of Fig. 5: 1, $g = 0.1 \times 10^{-20}$; 2, $g = 0.3 \times 10^{-20}$; 3, $g = 0.5 \times 10^{-20}$; 4, $g = 0.7 \times 10^{-20}$ J rad^{-2}. In contrast to the first case (Fig. 5), in this case electrostatic potential decreases with temperature monotonically. It is due to an increase of protonic relaxation time with temperature. Same as in the first case, at low temperatures the curves coincide, which is due to fast protonic relaxation. The lower the value of g, the more pronounced is hydrogen bond strain increase with temperature. Thus, the more rigid is a hydrogen bond, the wider is a temperature gap where the potential value is approximately constant. The relation between u_1 and u_2 determines the steepness of the transition to the case of highly strained hydrogen bond.

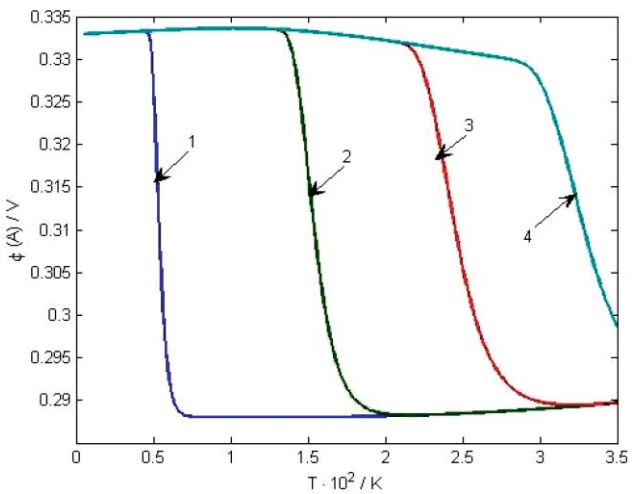

Fig. 6 The illustration of electrostatic potential $\varphi(A)$ temperature dependence at observation point A in case of hydrogen bond potential profile transition (c) → (d) (Fig. 4): $u_1 = 0.1$ eV → $u_2 = -0.05$ eV. An electron lifetime at electron accepting center, which limits the time of protonic relaxation equals $\tau_e = 0.1$ s. Different curves correspond to different hydrogen bond bending strain rigidity, just like in case of Fig. 5: 1, $g = 0.1 \times 10^{-20}$; 2, $g = 0.3 \times 10^{-20}$; 3, $g = 0.5 \times 10^{-20}$; 4, $g = 0.7 \times 10^{-20}$ J rad^{-2}. Contrary to the first case (Fig. 5), in this case electrostatic potential decreases with temperature monotonically, due to increase of protonic relaxation time with temperature. Same as in the first case, at low temperatures, when hydrogen bond strain is insufficient, the curves, corresponding to different values of g, coincide. The lower the value of g, the more pronounced is hydrogen bond strain increase with temperature. Upon reachingthe critical value of bond strain, the process of protonic relaxation slows down. This corresponds to descent to the values typical for the curves corresponding to small values of g.

Fig. 7 illustrates temperature dependence of electrostatic potential $\varphi(A)$ in case of $g = 0.5 \times 10^{-20}$ J rad^{-2}. The curves are presented for different relations between u_1 and u_2. In all cases the value of u_1 is the same and equals $u_1 = 0.1$ eV, while the value of u_2 varies from –0.05 eV to 0.05 eV: 1, $u_2 = 0.05$; 2, $u_2 = 0.02$; 3, $u_2 = 0.05$; 4, $u_2 = 0$; 5, $u_2 = -0.01$; 6, $u_2 = -0.02$; 7, $u_2 = -0.05$ eV. According to the figure, in the temperature gap from low temperatures up to the temperature of steep decrease the curves are symmetric relative to curve 4. This is a result of the mutual symmetry of u_1 and u_2 parameters. When temperature reaches the value which corresponds to the highly strained hydrogen bond (approximately 230 K in case of the used value of g), all four curve variations become the same. This results from protonic relaxation slow down, *i.e.* considerable relaxation time τ increase (Fig. 3).

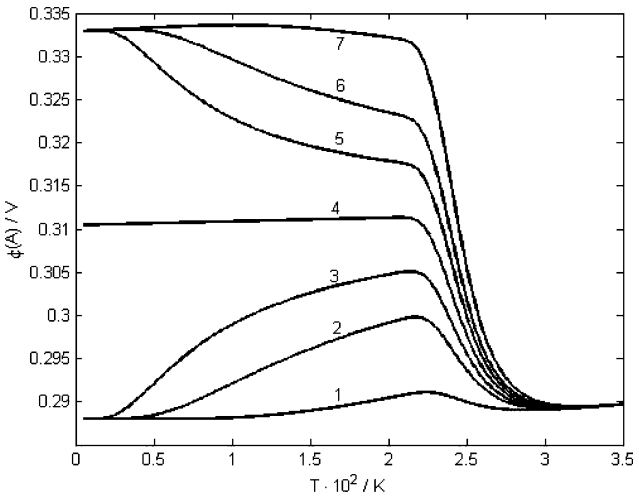

Fig. 7 Electrostatic potential $\varphi(A)$ temperature dependence at observation point A, which is 5 Å aside from the hydrogen bond proton (the angle $\alpha = 30°$), $g = 0.5 \times 10^{-20}$ J rad^{-2}. The curves are presented for different relations between u_1 and u_2. In all cases the value of u_1 is the same and equals $u_1 = 0.1$ eV, while the value of u_2 varies from –0.05 eV to 0.05 eV: 1, $u_2 = 0.05$; 2, $u_2 = 0.02$; 3, $u_2 = 0.05$; 4, $u_2 = 0$; 5, $u_2 = -0.01$; 6, $u_2 = -0.02$; 7, $u_2 = -0.05$ eV.

An interesting aspect of potential $\varphi(T)$ variation temperature dependence is the change of temperature value corresponding to steep transition, which depends on electron life time τ_e at electron accepting center. As we have noted above, this time confines the time of protonic relaxation. Since the time of protonic relaxation τ depends on temperature and rises with temperature increase (see Fig. 3b), at high temperatures the relaxation process can not be completed during the given period of time. Fig. 8 illustrates temperature dependence of electrostatic potential $\varphi(T)$ in different cases of electron life time at accepting center τ_e. Observation point A is located 5 Å aside of the hydrogen bond proton (angle $\alpha = 30°$), $g = 0.5 \times 10^{-20}$ J rad^{-2}. Presented curves correspond to the second type of change of hydrogen bond potential profile ((c) → (d), Fig. 4): $u_1 = 0.1$ eV → $u_2 = -0.05$ eV. Curves 1, 2, 3, 4, 5, 6 correspond the following values of τ_e: 10^{-3}, 10^{-2}, 10^{-1}, 1, 10, 10^2 s. Such a trend of curves is determined by the relation of electron life time at accepting center τ_e and relaxation time τ, which is also temperature dependent. For example, if the system temperature value equals 250 K, full relaxation takes about 1 s. Hence, if $\tau_e <$ 1 s at this temperature, the system will not reach its equilibrium

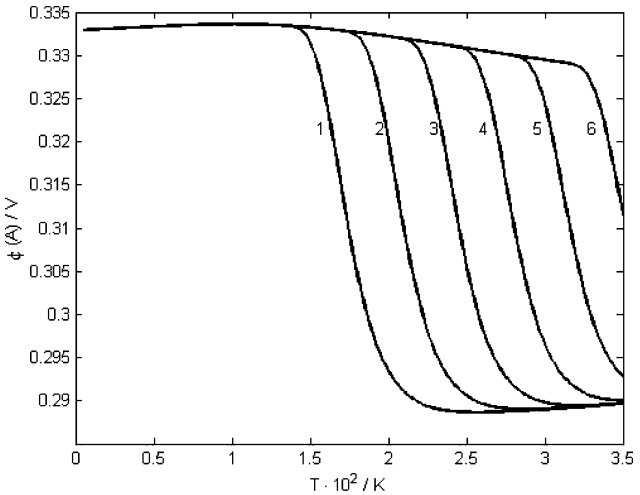

Fig. 8 Temperature dependence of electrostatic potential $\varphi(A)$ in different cases of electron life time at accepting center τ_e. Observation point A is located 5 Å aside of hydrogen bond proton (angle $\alpha = 30°$), $g = 0.5 \times 10^{-20}$ J rad^{-2}. Presented curves correspond to the second type of change of hydrogen bond potential profile ((c) → (d), Fig. 4): $u_1 = 0.1$ eV → $u_2 = -0.05$ eV. Curves 1, 2, 3, 4, 5, 6 correspond the following values of τ_e: 10^{-3}, 10^{-2}, 10^{-1}, 1, 10, 10^2 s.

state in terms of protonic relaxation, and the value of electrostatic potential at point A will not reach its maximal value.

III. The temperature dependence of reaction (1) free energy ΔG

Electrostatic potential $\varphi(A)$, generated by the molecular environment at electron localization area, makes a contribution to the system energy state by shifting electronic energy levels. This causes changes in system redox potential as well as free energy difference of various molecular processes. One such process is the reaction of recombination $P^+Q_A^- \rightarrow PQ_A$, which is an electron transfer from the primary quinone at the bacteriochlorophyll dimer within *Rhodobacter sphaeroides* RC. As it was noted in the introductory part of this paper, it is impossible to justify this reaction rate temperature dependence on the basis of conventional theoretical approaches. In order to achieve a compliance of calculated values with experimental ones, one should make some extra assumptions: either energy of reorganization λ, which accompanies this process, or free energy ΔG of this process is temperature dependent. Authors of papers devoted to the study of this problem, for example references 4 and 7, point out, that experimental data does not permit one to distinguish which of these parameters (either λ or ΔG) vary with temperature.

Now we turn to expression (13), which describes variation of the energy of electrostatic interaction between an electron, localized at point A, and partial charge at the hydrogen bond proton. Using eqn (12), (21)–(24) and the values of corresponding parameters one can calculate the shift of a system electronic level due to this interaction. The shift of the corresponding electronic level implies a change of midpoint redox potential of the system, *i.e.* change of reaction free energy ΔG. Since $\Delta\varphi(A)$ is temperature dependent, ΔG depends on temperature as well. According to (11) and (13) the temperature dependence alteration of free energy difference $\Delta G(T)$ is the following equation

$$\Delta G(T) = -(\Delta E_m^{\max} - \Delta E_m(T)), \tag{29}$$

where $\Delta E_m^{\max} = -e(\varphi_2 - \varphi_1)$. Using the equalities (12), (8) and also (21)–(24), one can obtain the explicit expression for $\Delta G(T)$.

Fig. 9 presents the experimental results[4] of reorganization energy $\lambda(T)$ temperature dependence (circles) and fit results for $\Delta G(T)$ using the expressions (12), (13), (8) and also (21)–(24) (solid lines). The following generally accepted parameter values were used: $|r| = 4$ Å, $\alpha = 0$ rad, $l = 1$ Å, $\varepsilon = 3$, $\nu = 10^{14}$ s^{-1}, $u_1 = 1$ eV. Other parameters have somewhat different values: $e_p = 0.46$ e, $u_{ph} = 0.01$ eV, $u_2 = -0.019$ eV, $g = 0.48 \times 10^{-20}$ J rad^{-2} and $d = 0.8$ Å (almost weak H-bond) (curve 1); $e_p = 0.52$ e, $u_{ph} = 0.01$ eV, $u_2 = -0.018$ eV, $g = 0.35 \times 10^{-20}$ J rad^{-2} and $d = 0.7$ Å (H-bond of medium strength) (curve 2); $e_p = 0.63$ e, $u_{ph} = 0.014$ eV, $u_2 = -0.016$ eV, $g = 0.27 \times 10^{-20}$ J rad^{-2} and $d = 0.6$ Å (strong short H-bond) (curve 3). Also it was taken in to account that the primary quinone Q_A forms two hydrogen bonds. As one can see, there is a quite good agreement between calculated and experimental values.

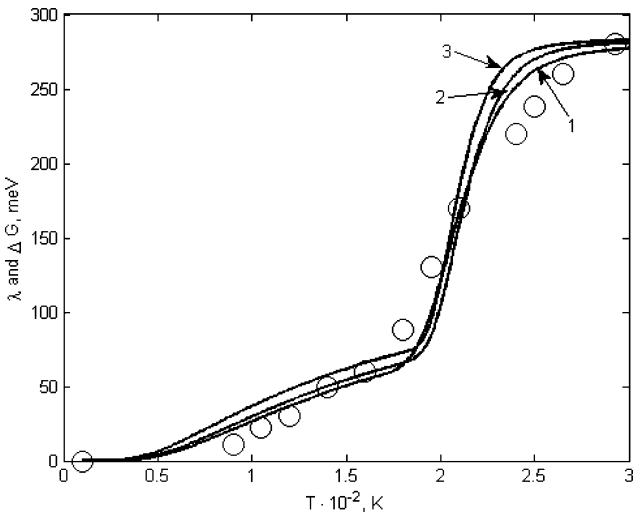

Fig. 9 The experimental results[4] of reorganization energy λ temperature dependence (circles) and fitting the results for $\Delta G(T)$ using the expressions (12), (13), (8) and also (21)–(24) (solid lines). The following common parameters values were used: $|r| = 4$ Å, $\alpha = 0$ rad, $l = 1$ Å, $\varepsilon = 3$, $\nu = 10^{14}$ s^{-1}, $u_1 = 1$ eV. Others parameters have different values: $e_p = 0.46$ e, $u_{ph} = 0.01$ eV, $u_2 = -0.019$ eV, $g = 0.48 \times 10^{-20}$ J rad^{-2} and $d = 0.8$ Å (almost weak H-bond) (curve 1); $e_p = 0.52$ e, $u_{ph} = 0.01$ eV, $u_2 = -0.018$ eV, $g = 0.35 \times 10^{-20}$ J rad^{-2} and $d = 0.7$ Å (H-bond of medium strength) (curve 2); $e_p = 0.63$ e, $u_{ph} = 0.014$ eV, $u_2 = -0.016$ eV, $g = 0.27 \times 10^{-20}$ J rad^{-2} and $d = 0.6$ Å (strong short H-bond) (curve 3).

Two comments are appropriate here:

1. According to experimental results[4] the rate constant value of electron transfer in reaction (1) varies from 44 s^{-1} (10 K) to 11 s^{-1} (293 K) (wild type RC). Hence, the characteristic time τ_e of this reaction lies between 0.023 s (10 K) and 0.09 s (293 K). The temperature dependence of the protonic relaxation time τ ($\log_{10}(\tau)$) for each $\Delta G(T)$ curve is presented in Fig. 10 (it is very interesting that all lines intersect in a single point near 220 K). It can be seen that $\tau << \tau_e$ if $T < 150$ K and, on the contrary, $\tau >> \tau_e$ when $T > 250$ K for all cases. Therefore, according to the standard classification the electron transfer process (1) is an

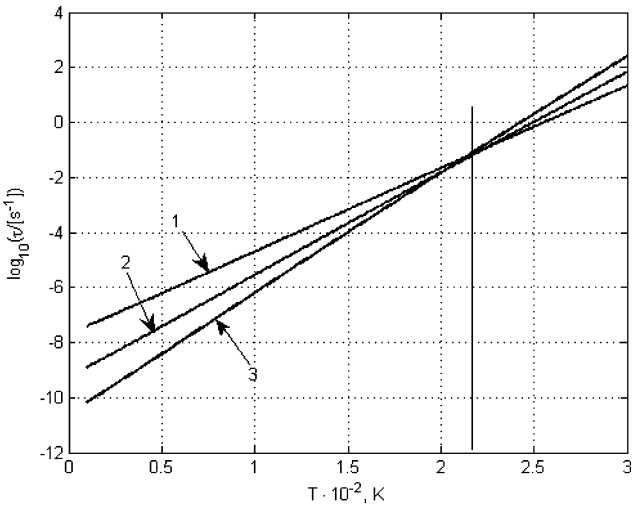

Fig. 10 The temperature dependence of relaxation time ($\log_{10}(\tau/[s])$ for different type of the hydrogen bonds: 1, almost weak H-bond (d = 0.8 Å); 2, H-bond of medium strength (d = 0.7 Å); 3, strong H-bond (d = 0.6 Å). For the values of others parameters see text or the legend to Fig. 9.

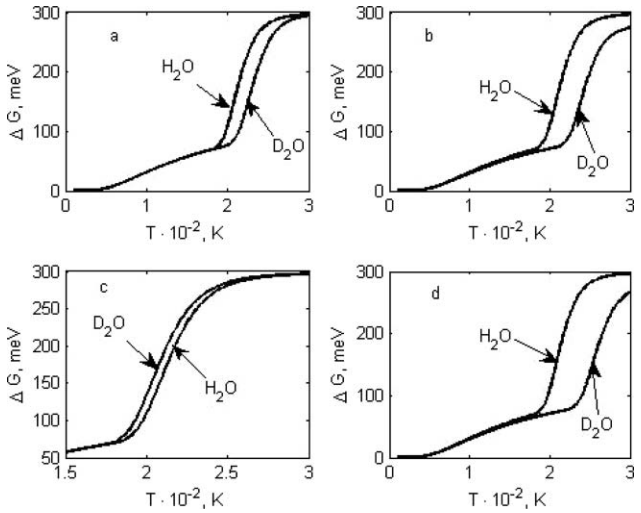

Fig. 11 Possible changes of ΔG temperature dependence in the case when protons are replaced by deuterons: (a) the right shift of the curve is caused by possible changing of the flexural rigidity of the hydrogen bond in D_2O only ($g_H = 0.5 \times 10^{-20}$ J rad^{-2} → $g_D = 0.55 \times 10^{-20}$ J rad^{-2}); (b) in this case also the right shift of curve takes place which is caused by possible changing of the distance between two minima of double well potential only ($d_H = 0.8$ Å → $d_D = 0.7$ Å); (c) the left shift of curve is caused by change of frequency only ($\nu_H \rightarrow \nu_D$ ($\nu_D = \frac{\nu_H}{\sqrt{2}}$)); in this case the magnitude of the shift is small and for better representation the temperature axis begins at 150 K; (d) in this case all factors affect the shift of the curve.

adiabatic process at T < 150 K and, in contrast; this process is non-adiabatic at T > 250 K. In the temperature gap from 150 to 250 K the intermediate dynamical regime takes place.

2. The effect of isotopic replacement H → D. It is well known that properties of hydrogen bonds can change if protons are replaced by deuterons. The more obvious of them is the proton vibration frequency (ν), which for deuteron is decreased $\sqrt{2}$ times as small. It was already noted above. The rigidity of H-bonds (g) and the distance between minima of double well potential (d) of these bonds also can change. According to literature data,[17,18] these parameter values can vary by about 5–10%. Let us accept, for example, that the rigidity is changed as: $g_H = 0.5 \times 10^{-20}$ J rad^{-2} → $g_D = 0.55 \times 10^{-20}$ J rad^{-2} and also $d_H = 0.8$ Å → $d_D = 0.76$ Å. Fig. 11 demonstrates possible changes of $\Delta G_D(T)$ curve (labeled by D_2O) in comparison to $\Delta G_H(T)$ curve labeled by H_2O). For the last, the following values of parameters were accepted: |r| = 3.6 Å, $\alpha = 0$ rad, $\varepsilon = 3.5$, $\nu = 5 \times 10^{13}$ s^{-1}, $\tau_e = 0.05$ s, $g = 0.5 \times 10^{-20}$ J rad^{-2}, $u_{ph} = 0.0026$ eV, $u_1 = 1$ eV, $u_2 = -0.018$ eV. In Fig. 11a the right shift caused by changes of g parameter only is shown: $g_H = 0.5 \times 10^{-20}$ J rad^{-2} → $g_D = 0.55\ 10^{-20}$ J rad^{-2}. In Fig. 11b the right shift caused by change of d parameter only is shown: $d_H = 0.8$ Å → $d_D = 0.76$ Å. In Fig. 11c the small left shift caused by change of ν frequency only is shown: $\nu_H \rightarrow \nu_D$ ($\nu_D = \frac{\nu_H}{\sqrt{2}}$). Finally, in Fig. 11d the total effect of all these factors is shown. It leads to the qualitative conclusion that the rate constant of electron transfer reaction (1) in *R. sphaeroides* RC with D_2O ($k_e|_D(T)$) would be some what higher in comparison to H_2O ($k_e|_H(T)$) at $T > 180$ K. This conclusion is in agreement qualitatively with experimental observations.[24]

IV. Discussion

Above we have discussed one of the possible relaxation mechanisms in a molecular system, which is due to proton redistribution between two stable positions within a hydrogen bond double well potential. This redistribution occurs due to changes of hydrogen bond double well potential, caused by changes of the electronic state of a molecular system. A feature of the relaxation process is that it takes place due to tunneling of protons along hydrogen bonds and its efficiency depends essentially on hydrogen bond bending strain, since it causes an increase in the efficient distance between double well potential minima. The temperature rise causes the increase in hydrogen bonds bending strain due to the increase in atom thermal motion enhancement. Due to this process, the efficiency of protons redistribution decreases abruptly. Hence, the temperature rise slows down this relaxation process, since, contrary to the activation processes, it is due to proton tunneling along hydrogen bonds.

The most important factor which determines the magnitude of the effect is a change of a hydrogen bond potential energy profile due to the change of the system electronic state, which implies either the appearance or disappearance of an electron in the electron localization area. The most probable effect of an electron appearance at the localization area (*i.e.* acceptor reduction) is a deepening of the potential well minimum closest to the electron localization area (Fig. 5). We considered this case analyzing the reorganization energy temperature dependence, presented in Fig. 9. At the same time we can not exclude other possibilities, as noted above. Depending on the particular situation, the equilibrium value of the system redox potential can be either higher or lower than its initial value. This also determines the trend of the temperature dependence $\varphi(T)$. According to Fig. 5, the trend of this curve may be non-monotonic, while preserving the general tendency to increase the potential with the temperature rise. Another case corresponds to the temperature dependence presented in Fig. 6. In this case the steep decrease occurs in the narrow temperature gap, while at other temperatures the value of the potential is almost constant.

The important question is whether the realization of the suggested mechanism in RC of *Rhodobacter spaeroides* is really possible? As it is clear from the above material, the protonic relaxation mechanism only takes place in the double well potential hydrogen bond. Are H-bond potentials between Q^-_A and HisM219 and AlaM260 double well potentials? Recently it has been found that the H-bond between Q^-_A and HisM219 is strong, hence, according to the standard classification, this H-bond is quite likely to be a single well potential.

The standard classification of the hydrogen bonds is based on its strength and includes strong, medium and weak H-bonds. The strong type of the H-bond is represented by a single well potential or double well potential with low barrier. The distance between heavy atoms of strong H-bond lies between 2.1 and 2.6 Å whereas the hydrogen bond distance (H ⋯ B) ranges from 1.2 to 1.6 Å. Hence, the parameter d which denotes the distance between minima of double well potential should be d ≤ 0.6 Å. The medium type of the H-bond is represented by highly anharmonic single well potential compared to the non-hydrogen-bonded system. The distance between heavy atoms in this case lies between 2.4 and 3.3 Å whereas the hydrogen bond distance ranges from 1.5 to 2.2 Å. Hence, the parameter d ranges from 0.5 to 1.2 Å approximately. In the weak hydrogen bonds the potential is characterized by an asymmetric double minimum in the general case. The distance between heavy atoms is between 3.1 and 4.3 Å, whereas the hydrogen bond distance ranges from 2.2 to 3.2 Å. Hence, parameter d roughly ranges from 1.1 to 2.3 Å.

This classification presupposes that heavy atoms (or atomic groups) of the H-bond are neutral (A–H ⋯ B). However, if the electronic state of the one of two heavy atoms changes then the form of H-bond potential can essentially change in comparison to the initial state (for example, in the case A–H ⋯ B^-). Therefore, even if the H-bond is strong and has a single well potential curve in a neutral state it does not mean that the form of this potential will be retained as a single well after the change of the electronic state of the molecular system. Moreover, there are many neutral molecular structures with the strong and double well potential H-bonds. For example, in the Zundel's ion $H_5O_2^+$ or potassium hydrogen carbonate ($KHCO_3$) crystal the length of the H-bonds is 1.6 Å, nevertheless these H-bonds have the double well potential.[26] It has been found that the compound 4-cyano-2,2,6,6-tetramethyl-3,5-heptanedione has the shortest symmetrical O–H ⋯ O hydrogen bond with a double well potential.[27] It also has been found[28] that the proton occupies an asymmetric, double-well position between oxygen atoms, confirming one of the shortest asymmetric hydrogen bonds known in minerals with $R_{OO} = 2.464$ Å.

In reference 21 it was found that in the neutral state the distance R(O ⋯ H) is equal to 2.05 Å for Ala and 1.9 Å for His whereas in the reduced state (Q^-_A) the distance R(O ⋯ D) is equal to 1.73 and 1.6 Å, correspondingly. The geometry of both of these H-bonds is non-linear and the form of the H-bond potential energy surface can not be measured experimentally. It is very interesting to compare these results with other experimental data, which was published recently.[23] For example, it has been shown that the head group of Q_A^- undergoes a 60° rotation in the ring plane relative to its orientation in the crystal structure (*i.e.* X-ray data). This result[23] contradicts to the previous result.[21] Indeed, such rotation means that the H-bond between Q^-_A and His is broken and it may be that the H-bond between Q^-_A and Ala is broken too. At the same time, according to reference 21 these H-bonds are present in the Q^-_A state and, furthermore, are strong ones. We think that future studies are needed to reveal the nature of the H-bond between Q^-_A and HisM219 and if it is a single well potential bond only.

In our *ab initio* calculations[11,25] of the Q_A molecular model it was shown that in the neutral state both H-bond potentials between Q_A and HisM219 and between Q_A and AlaM260 are medium asymmetric single well potentials. However, after the reduction of Q_A ($Q_A \rightarrow Q^-_A$), potentials of both of these bonds transform to the double well potentials and moreover the distance between heavy atoms becomes shorter by 0.1 Å (2.8 → 2.7 Å). The angle in N–H ⋯ O is about 160° in both cases. The possibility to apply the suggested protonic relaxation mechanism to concrete RC *R. sphaeroides* processes was suggested on the ground of our computational results.[11,25]

The P dimer is the second partner in the recombination reaction $P^+Q_A^- \rightarrow PQ_A$. This cofactor has one H-bond with His L168 in the wild type RC. We carried out *ab initio* calculations of the two molecular models: (P ⋯ H–HisL168) (1) and (P^+ ⋯ H–HisL168) (2) (atomic coordinates for the all RC's molecules were obtained from RCSB Protein Data Bank (PDB ID: 1AIJ)). In both cases the H-bond potential is essentially a single well potential (unpublished). It is quite clear that the energy of the ion pair state (P–H^+ ⋯ His^-) is higher than the initial state (P ⋯ H–His) (model (1)). This energy would be yet higher for the state (P^+–H^+ ⋯ $^-$His) in comparison the initial state (P^+ ⋯ H–His) (model (2)). For the H-bonds of the mutant RC the situation is obviously the same. Since the protonic relaxation mechanism takes place only in the double well potential we didn't consider these H-bonds here.

Of course, an important role in this process belongs to protons of hydrogen bonds formed by the electron accepting center with its environment. However, it is quite likely that remote hydrogen bonds, for example those within water clusters,[22] can also contribute. The electrostatic potential variation depends on the hydrogen bond orientation relative to the electron localization center and the distance r between the latter and the protons of H-bonds. Evidently, the major effect is due to the radially oriented hydrogen bonds. The total effect from the remote H-bonds can be a large enough.

Charge recombination occurs at a different temperature than charge separation. The difference between the two cases concerns the initial state of the molecular system. In our model the initial state is defined by the population value $n_1(0,T)$. In the initial (*i.e.* neutral) state the H-bond potential is the asymmetric single well potential, *i.e.* the parameter value $u_1 > 1$ eV. Hence, $n_1(0,T) = 1$ for any temperature. However, it is known[5] that the cooling of the RC in the light or in the dark from room temperature to cryogenic temperature produces different electron transfer rate constant values $k_e(T)$ of the reaction (1) and $k_e(T =$ cryogenic) for cooling in the light RC approximately equals to $k_e(T =$ room). It evidences conformation changes in the molecular structure of the RC. The nature of possible conformation modifications in the quinone site of RC *R. sphaeroides* are unknown and studied actively now.[23] If the conformation change modifies the quinone's H-bonds (and others) then such modification can be considered by our theory. Indeed, the conformation change deforms of H-bond and changes the parameter values d, u_1, u_2 and some others, and hence, n_1 and n_2 change as well. If, for example, there are two stable conformation states then it will be the two equilibrium values of

d_1 and d_2. In this case the protonic relaxation mechanism occurs coupled to the conformation relaxation, which can be described using eqn (25)–(28). However, it is important to indicate concrete conformation changes in the molecular structure of RC. Now we continue *ab initio* calculations of a model molecular system of the quinone's site RC. Our model computations revealed possible conformational transfer in the molecular structure of the quinone's environment following transition $Q_A \rightarrow Q^-_A$. However, the results should be verified and therefore we haven't discussed in detail this question now. It is also important for the interpretation of the mechanism of electron forward reaction $Q^-_A Q_B \rightarrow Q_A Q^-_B$. For example, this problem has been discussed in reference 23. It is noteworthy that reactions $P^+Q^-_A \rightarrow PQ_A$ and $Q^-_A Q_B \rightarrow Q_A Q^-_B$ are not coupled directly since the first reaction ends before the second reaction starts at any temperature.

The third aspect which we want to discuss concerns a correlation between λ and ΔG. The change of the system electronic state brings about the appearance of the H-bond double well potential and causes some shift of the equilibrium position of the initial potential well minimum. Taking to the account that the frequency of proton vibrations within a potential well equals approximately to 10^{14} s^{-1} (~3300 cm^{-1}), this shift can be referred to as a reorganization process of high frequency vibration modes in the nuclear subsystem of a total molecular structure. According to our computations,[11] for the quinone's H-bond this shift equals approximately to $\Delta x \approx 0.16$ Å. Using the well known expression $\lambda = \hbar\omega S = \hbar\omega \frac{1}{2}\left(\frac{\Delta x}{x_0}\right)^2$, where x_0 is the magnitude of the zero-point oscillations, the estimation $\lambda \equiv \lambda_L \approx 530$ meV is valid. Note, in reference 4 the value of the high frequency part of the reorganization energy is estimated as $\lambda_L = 650$ meV but the frequency is equal to 1600 cm^{-1}. This part of the reorganization energy is temperature independent.

At the same time proton redistribution itself means that the proton positions change. This reorganization occurs due to the interaction with environment, which provides the energy compensation equal to the energy $\lambda_M = u_2$. Therefore, parameter u_2 can be considered as low frequency part of the reorganization energy. At the same time the efficiency of the proton redistribution process depends on the H-bond deformation, which in its turn depends on temperature. Hence, it suggests that the protonic relaxation process is a low frequency process of the medium reorganization. It is necessary to note that the temperature dependence of this reorganization process is determined by the temperature dependence of the relaxation time $\tau(T)$. In our model $\lambda_M = u_2 \approx 20$ meV. Hence, the total reorganization energy is $\lambda = \lambda_L + \lambda_M \approx 550$ meV.

The change of the electrostatic potential at electron localization area, due to proton redistribution within the double well potential of hydrogen bonds, causes the shift of the system electronic level. It implies the change of the system redox potential, *i.e.* the change of the free energy of the existing state. The temperature dependence of the free energy difference, presented in Fig. 9, corresponds to the temperature dependence of electrostatic potential at the electron localization area, presented in Fig. 6. According to Fig. 6, the absolute value of the electrostatic energy of the interaction between hydrogen bonds protons and an excessive electron $\Delta E = |e\varphi(T)|$ decreases with the temperature rise. This implies the decrease of the system redox potential (its electronic level shifts upwards). As a result the free energy of the recombination (1) increases.

There is some doubt concerning the interpretation of the reorganization energy itself. For example authors of reference 4 note the following. If one supposes that an interaction that stabilizes the state with separated charges increases with temperature, then λ should decrease and $-\Delta G$ should rise with temperature. On the other hand, the same authors state that their experimental data can be fitted using conventional theory, if one uses a single normal mode 1600 cm^{-1}, under the assumption that λ decreases by several hundred meV with the temperature rise. It will be recalled that the experimental points, plotted in Fig. 9, were published in paper[4] and correspond to two-mode approximation of the theory in which the reorganization energy rises with temperature. The mechanism of protonic relaxation, discussed in our paper, corresponds to the interaction, which stabilizes an electron at the accepting center with the temperature decrease.

Appendix A

In order to find time dependence of these states, we consider the non-stationary Schroedinger equation with Hamiltonian (17)

$$i\hbar\frac{\partial\psi}{\partial t} = \hat{H}\psi. \tag{A1}$$

We express wave function ψ as a linear combination

$$\psi(t) = a_1(t)\psi_1 + a_2(t)\psi_2, \tag{A2}$$

of wave functions (16), taking into account phase factor

$$\begin{aligned}\psi_1 &= \psi_1(\xi,t) = \psi_1(\xi)\exp\left(-i\frac{\varepsilon_0}{\hbar}t\right),\\ \psi_2 &= \psi_2(\xi,t) = \psi_2(\xi)\exp\left(-i\frac{\varepsilon_0}{\hbar}t\right).\end{aligned} \tag{A3}$$

Coefficients $a_j(t)$ in states superposition (A2) are the weight factors that determine the probability $p_j(t)$ of state ψ_j realization: $p_j(t) = |\alpha_j(t)|^2$. These coefficients are related due to the normality condition:

$$|a_1|^2 + |a_2|^2 = 1 \tag{A4}$$

The condition $a_1 = 1, a_2 = 0$, corresponds to proton localization within the first well, and condition $a_1 = 0, a_2 = 1$ to proton localization within the second potential well. Intermediate conditions correspond to proton delocalization between the wells.

Now we substitute (A2) into (A1), and multiply the result by ψ^*_1, and integrate both parts of the equation over the spatial variable ξ. Next we repeat the same manipulations except we multiply (A1) by ψ^*_2. After these manipulations we arrive to the following system of algebraic equations (here point denotes dime derivative)

$$\begin{cases} i\hbar(1+S)(\dot{a}_1 + S\,\dot{a}_2) = a_1V_{11} + a_2V_{12},\\ i\hbar(1-S)(\dot{a}_1 + S\,\dot{a}_2) = a_1V_{21} + a_2V_{22},\end{cases} \tag{A5}$$

where we use the following notation for matrix elements:

$$V_{ij} = \int_0^\infty \psi_i^*(U_2 - U_1)\psi_j d\xi \tag{A6}$$

and for overlap integral holds:

$$S = \int_0^\infty \psi_i^* \psi_j d\xi. \quad \text{(A7)}$$

Pay attention, that we integrate expressions (A6) and (A7) using limits [0, ∞), and the difference equals $U_2 - U_1 = -2\hbar\omega\delta\xi$. Due to symmetry of the potential (14), the following relations between matrix elements hold: $V_{11} = V_{22}$, $V_{12} = V_{21}$. Using these equalities and starting conditions $\alpha_1(0) = 1$, $\alpha_2(0) = 0$, one can easily find the solution of the system of eqn (A5). The expressions for probabilities $p_j(t)$ follow:

$$\begin{cases} p_1(t) = |a_1|^2 = \frac{1}{2}(1 + \cos(\Omega t)), \\ p_2(t) = |a_2|^2 = \frac{1}{2}(1 - \cos(\Omega t)), \end{cases} \quad \text{(A8)}$$

where Ω denotes the frequency of proton quantum oscillations between states ψ_1 and ψ_2 (the so-called Rabi frequency)

$$\Omega = \frac{V_{11} - V_{12}}{\hbar(1 - S^2)}. \quad \text{(A9)}$$

As one can see from the expression (A8), the probability of realization of state ψ_j, which corresponds to proton localization within the j-th well, varies periodically between 0 and 1 with time period $\tau_0 = \pi/\Omega$. Hence the probability of proton transition between the wells per time unit can be expressed as follows

$$k_0 = \frac{1}{\tau_0} = \frac{V_{11} - V_{12}}{\pi\hbar(1 - S^2)}. \quad \text{(A10)}$$

After evaluation of the integrals (A6) and (A7) using functions (16), and assuming the overlap integral S to satisfy the condition $S = \exp(-\delta^2) \ll 1$, which is almost always true, one can express the final result as follows

$$k_0 \approx \frac{2\nu}{\sqrt{\pi}} \delta \times \exp(-\delta^2), \quad (28)$$

where $\nu = \omega/2\pi$ denotes frequency of proton linear oscillations within a well, and $\delta = \frac{d/2}{x_0}$. Note that the same result for the k_0 was obtained using different approach in reference 19.

Acknowledgements

We thank Peter A. Mamonov for fruitful discussions. This study was supported by the Russian Foundation for Basic Research: project 07-04-00212.

References

1 J. Deisenhofer, O. Epp, K. Miki, R. Huber and H. Michel, X-ray structure analysis of a membrane protein complex. Electron density map at 3 Å resolution and a model of the chromophores of the photosynthetic reaction center from Rhodopseudomonas viridis, *J. Mol. Biol*, 1984, **180**, 385–389.
2 J. P. Allen, G. Feher, T. O. Yeates, H. Komiya and D. C. Rees, Structure of the reaction center from Rhodobacter sphaeroides R-26, *Proc. Natl. Acad. Sci. USA*, 1987, **84**, 5730–5734& 6162–6166, 1988, **85**, 8487–8491.
3 G. Feher, J. P. Allen, M. Y. Okamura and D. C. Rees, Structure and function of bacterial photosynthetic reaction centers, *Nature*, 1989, **339**, 111–116.
4 J. M. Ortega, P. Mathis, J. C. Williams and J. P. Allen, Temperature dependence of the reorganization energy for charge recombination in the reaction center from Rhodobacter sphaeroides, *Biochemistry*, 1996, **35**, 3354–3361.
5 B. H. McMahon, J. D. Muller, C. A. Wright and G. U. Nienhaus, Electron transfer and protein dynamics in the photosynthetic reaction center, *Biophysical Journal*, 1998, **74**, 2567–2587.
6 V. V. Gorbach, E. P. Lukashev, P. P. Knox, A. I. Komarov, A. A. Kononenko, V. N. Verkhoturov, E. G. Petrov and A. B. Rubin, Kinetics of bacteriochlorophyll and the primary quinone acceptor ion-radicals recombination in the photosynthetic reaction centers, *Izv. AN SSSR, ser. biol. (Russ.)*, 1986, **31**, 11–23.
7 R. Schmid and A. Labahn, Temperature and free energy dependence of the direct charge recombination rate from the secondary quinine in bacterial reaction centers from Rhodobacter sphaeroides, *J. Phys. Chem. B*, 2000, **104**, 2928–2936.
8 B. J. Hales, Temperature dependence of the rate of electron transport as a monitor of protein motion, *Biophys. J*, 1976, **16**, 471–480.
9 J. Jortner, Dynamics of electron transfer in bacterial photosynthesis, *Biochim. Biophys. Acta*, 1980, **594**, 193–230.
10 R. A. Marcus and N. Sutin, Electron transfers in chemistry and biology, *Biochim. Biophys. Acta*, 1985, **811**, 265–322.
11 P. M. Krasilnikov, P. A. Mamonov, P. P. Knox, V. Z. Paschenko and A. B. Rubin, The influence of hydrogen bonds on electron transfer rate in photosynthetic RCs, *Biochim. Biophys. Acta*, 2007, **1767**, 541–549.
12 X. Lin, H. A. Murchison, V. Nagarajan, W. W. Parson, J. P. Allen and J. C. Williams, Specific alternation of the oxidation potential of the electron donor in reaction centers from Rhodobacter sphaeroides, *Proc. Natl. Acad. Sci. USA*, 1994, **91**, 10265–10269.
13 A. L. M. Haffa, S. Lin, E. Katilius, J. C. Williams, A. K. W. Taguchi, J. P. Allen and N. W. Woodbury, The dependence of the initial electron-transfer rate on driving force in Rhodobacter sphaeroides reaction centers, *J. Phys. Chem B*, 2002, **106**, 7376–7384.
14 J. Rautter, F. Landzian, C. Schulz, A. Fetsch, M. Kuhn, X. Lin, J. C. Williams, J. P. Allen and W. Lubitz, ENDOR studies of the primary donor cation radical in mutant reaction centers of Rhodobacter sphaeroides with altered hydrogen-bond interaction, *Biochemistry*, 1995, **34**, 8130–8143.
15 I.-J. Lin, E. B. Gebel, T. E. Machonkin, W. M. Westler and J. L. Markley, Changes in hydrogen-bond strengths explain reduction potentials in 10 rubredoxin variants, *Proc. Natl. Acad. Sci. USA*, 2005, **102**, 14581–14586.
16 X. Yang, S. Niu, T. Ichiye and L.-S. Wang, Direct measurement of the hydrogen-bonding effect on the intrinsic redox potentials of [4Fe-4S] cubane complexes, *J. Am. Chem. Soc.*, 2004, **126**, 15790–15794.
17 G. C. Pimentel, A. L. McClellan, *The hydrogen bond*, WH Freeman and Co., San Francisco and London, 1960.
18 G. Zundel, *Proton polarizability of hydrogen bonds and proton transfer processes, their role in electrochemistry and biology*, Institute fur Physikalische Chemie der Universitat Munchen, 1997, 250 p.
19 J. A. Sussmann, Phonon induced tunneling of ions in solids, *Phys. Kondens. Materie.*, 1964, **2**, 146–160.
20 F. Cordier and S. Grzesiek, Temperature–dependence of protein hydrogen bond properties as studied by high-resolution NMR, *J. Mol. Biol*, 2002, **715**, 739–752.
21 M. Flores, R. Isaacson, E. Abresch, R. Calvo, W. Lubitz and G. Feher, Protein–cofactor interactions in bacterial reaction centers from Rhodobacter sphaeroides R-26: II. Geometry, of the hydrogen bonds to the primary Quinone Q_A^{-1}H and ^{2}H ENDOR spectroscopy, *Biophys. J*, 2007, **92**, 671–682.
22 U. Ermler, G. Fritzsch and H. Michel, Crystal structure of the reaction centre from *Rhodobacter sphaeroides* to 2.65 Å: Cofactors and Protein-Cofactor Interactions, *Structure*, 1994, **2**, 925–936.
23 U. Heinen, L. M. Utschig, O. G. Poluectov, G. Link, E. Ohmes and G. Kothe, Structure of the Charge Separated State $P_{865}^+Q_A^-$ in the Photosynthetic Reaction Centers of *Rhodobacter sphaeroides* by Quantum Beat Oscillations and High-Field Electron Paramagnetic Resonance: Evidence for Light-Induced Q_A^- Reorientation, *J. Am. Chem. Soc*, 2007, **129**, 15935–15946.
24 P. M. Krasilnikov, P. P. Knox, V. Z. Paschenko, G. Renger and A. B. Rubin, Relaxation processes: implication for the temperature dependence of the rate of reduction of photooxidized bacteriochlorophyll

by primary quinine in Rhodobacter sphaeroides reaction centers, *Biophysics*, 2002, **47**, 445–451.
25 P. M. Krasilnikov and P. A. Mamonov, Effect of hydrogen bonds on the energetic of macromolecules in the course of electron transfer, *Biophysics*, 2006, **51**, 226–232.
26 F. Fillaux, Hydrogen bonding and quantum dynamics in the solid state, *Int. Rev. in Physical Chemistry*, 2000, **19**, 553–564.
27 J. A. Belot, J. Clark, J. A. Cowan, G. S. Harbison, A. I. Kolesnikov, Y.-S. Kye, A. J. Schultz, C. Silvernail and Z. Xingang, The shortest symmetrical O—H · · · O hydrogen bond has a low-barrier double-well potential, *J. Phys. Chem*, 2004, **108**((B)), 6922–6926.
28 S. Jacobsen, J. R. Smyth, R. J. Swope and R. I. Sheldon, Two proton positions in the very strong hydrogen bond of serandite, $NaMn_2[Si_3O_3(OH)]$, *American Mineralogist*, 2000, **85**, 745–752.